Proceedings of the 2001 IEEE
International Conference on Robotics & Automation
Seoul, Korea • May 21-26, 2001

Task-based Compliance Planning for Multi-Fingered Hands

Byoung-Ho Kim°,†, Byung-Ju Yi°, Sang-Rok Oh†, and Il Hong Suh°

° : School of Electrical Eng. and Computer Science, Hanyang Univ., Seoul, Korea
† : Intelligent System Control Research Center, KIST, Seoul, Korea
(E-mail: bj@email.hanyang.ac.kr)

Abstract

Based on the analysis of the stiffness relation between the operational space and the fingertip space of multi-fingered hands, this paper provides a guideline of task-based compliance planning for multi-fingered hands. Two- and three-dimensional examples are illustrated to show the characteristics of the task-based stiffness matrix. It is shown that some of coupling stiffness elements cannot be planned arbitrarily due to grasping geometry. Through the analytical results, it is concluded that the operational stiffness matrix should be carefully specified by considering the location of compliance center and the grasp geometry of multi-fingered hands for successful grasping and manipulation tasks.

Keywords : *multi-fingered robot hand, compliance control, compliance planning*

1 Introduction

Recently, there are proposed several explicit force-based control techniques for effective grasping and manipulation of object by multi-fingered hands, or multiple robot arms[1]-[3]. Implementation of those methods may suffer from attaching force sensors in relating small finger mechanisms, as well as processing noisy force signals. Also, the integration of tactile and force information for individual finger control, and the combination of information from different fingers to guide the hand action are not still well-known[4]. Thus,instead of employing force signals, stiffness or compliance as successful alternatives has been known to be useful for characterizing the grasping and manipulation of robot hands[5][6]. Specially, when an object grasped by multi-fingered hand is being manipulated in constrained space, the appropriate compliance planning of the hand may be crucial for successful compliant tasks[7]-[9].

Related to grasp stiffness or compliance, Cutkosky et al.[5] analyzed the effective grasp stiffness by considering the structural compliances in fingers and fingertips, servo gains at the joints of finger, and small changes in the grasp geometry that may affect the grasp forces acting upon the object. Also, Kao, et al.[6] tried to apply stiffness models usually employed in robotics research to the analysis of human grasping behaviors. Kim, et al.[10] proposed an independent finger/joint-based compliance control method for robot hands manipulating an object, and also the geometric condition for successful implementation of compliance control scheme have been addressed. They showed that an independent finger/joint-based compliance control via redundant actuation was more adequate to modulate the operational stiffness comparing with the case of the kinematically redundant structured fingers or manipulators. Some researchers have investigated the task-based stiffness characteristics with respect to the task motion constraints[11]-[13]. They pointed out that the diagonal stiffness elements can be determined by considering the task characteristics for each direction. In [14], task-based compliance planning was presented. However, their approach is based on passive compliance attached to manipulator, but not related to multi-fingered hands. It is also pointed out that a stiffness matrix containing some off-diagonal terms can be useful to prevent jamming of contact tasks. In [15], fundamentals of compliance characteristics for multi-fingered hands has been analyzed. It was shown that some of coupling stiffness elements cannot be planned arbitrarily, and a five-fingered hand is necessary to modulate 6×6 operational stiffness matrix by using an independent finger-based compliance control method which is effective to achieve the specified compliance characteristics. They also pointed out that the operational stiffness matrix should be carefully specified in consideration of the grasp geometry of multi-fingered hands for successful grasping and manipulation tasks. However, task-

based analysis for specifying compliance characteristics by considering the grasp geometry and the compliance center is still an open research field.

The objective of this paper is to provide task-based guideline for specifying compliance characteristics of multi-fingered hands through investigation of the stiffness relation between the operational space and the fingertip space. In section 2, we treat two-dimensional compliance planning for many cases of robotic tasks. And then, compliance planning in the three-dimensional space is analyzed in section 3. Finally, concluding remarks are drawn in section 4.

2 Specifying Compliance Characteristics: Two-dimension

In this section, through investigation of the stiffness relation between the operational space and the fingertip space, we present a guideline to appropriately specify compliance characteristics in the operational space in comparison of the location of compliance center and the grasp geometry.

2.1 *Straight Peg*

When an object is assembled by multi-fingered hands as shown in Figure 1, the performance of the given task is closely related to the grasp geometry and the location of compliance center.

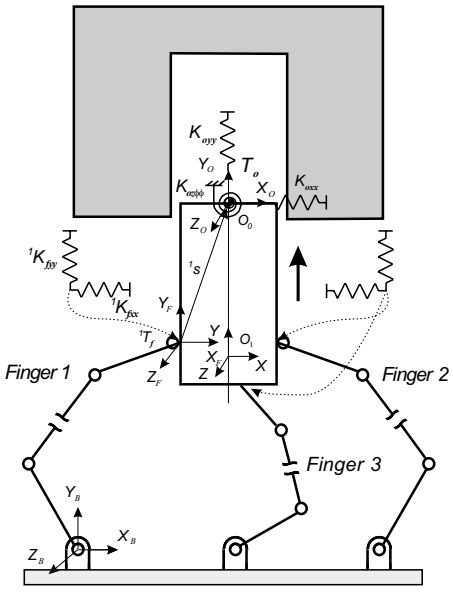

Figure 1: Peg-in-hole task using multi-fingered hands (straight peg)

In multi-fingered hand system, the stiffness relation between the operational space and the fingertip space is given by

$$[\boldsymbol{K}_o] = [\boldsymbol{G}_o^f]^T [\boldsymbol{K}_f][\boldsymbol{G}_o^f], \tag{1}$$

where $[\boldsymbol{K}_o]$ and $[\boldsymbol{K}_f]$ denote the stiffness matrix in the operational space and the fingertip space, respectively. $[\boldsymbol{G}_o^f]$ denotes the Jacobian matrix relating the fingertip space to the operational space.

In (1), the Jacobian matrix $[\boldsymbol{G}_o^f] \in \mathcal{R}^{m\times n}$ is given by

$$[\boldsymbol{G}_o^f] = \left[\begin{array}{cccc} [^1\boldsymbol{G}_o^f]^T & [^2\boldsymbol{G}_o^f]^T & \cdots & [^{n_f}\boldsymbol{G}_o^f]^T \end{array} \right]^T,$$

$$[^i\boldsymbol{G}_o^f] = \left[\begin{array}{cc} {}_o^f\boldsymbol{R}_i & {}_o^f p_i \times {}_o^f\boldsymbol{R}_i \\ 0 & {}_o^f\boldsymbol{R}_i \end{array} \right],$$

where ${}_o^f\boldsymbol{R}_i$ and ${}_o^f p_i$ denotes the rotation matrix and the position vector from the operational space to the fingertip space, respectively. Also, $m(m = \sum_{i=1}^{n_f} {}^i n_{fp}$, where ${}^i n_{fp}$ denotes the dimension of the ith fingertip) denotes the total dimension of wrenches applied to the grasped object by n_f fingers.

Also, the desired compliance characteristics in the operational space can be achievable by solving the following linear programming problem[15]:

$$K_{oo} = [\boldsymbol{B}_f^o]\, K_{ff}, \tag{2}$$

subject to $K_{ff} \geq 0$. In (2), K_{oo} and K_{ff} denote the independent stiffness elements of the operational space and the fingertip space, respectively. $[\boldsymbol{B}_f^o]$ denotes the stiffness mapping matrix relating the operational space to the fingertip space.

First, consider the compliance center lying in the point $\boldsymbol{O}_1$ of Figure 1. The independent stiffness relation between the operational space and the fingertip space is given by

$$\begin{aligned} K_{oo} &= [\boldsymbol{B}_f^o]\, K_{ff} \\ &= \left[\begin{array}{cccccc} 1 & 0 & 1 & 0 & 1 & 0 \\ 0 & 0 & 0 & 0 & 0 & 0 \\ -y_1 & 0 & -y_2 & 0 & y_3 & 0 \\ 0 & 1 & 0 & 1 & 0 & 1 \\ 0 & -x_1 & 0 & x_2 & 0 & x_3 \\ y_1^2 & x_1^2 & y_2^2 & x_2^2 & y_3^2 & x_3^2 \end{array} \right] K_{ff} \end{aligned} \tag{3}$$

where

$$K_{oo} = [\boldsymbol{K}_{oxx}\ \boldsymbol{K}_{oxy}\ \boldsymbol{K}_{ox\phi}\ \boldsymbol{K}_{oyy}\ \boldsymbol{K}_{oy\phi}\ \boldsymbol{K}_{o\phi\phi}]^T,$$
$$K_{ff} = \left[{}^1\boldsymbol{K}_{fxx}\ {}^1\boldsymbol{K}_{fyy}\ {}^2\boldsymbol{K}_{fxx}\ {}^2\boldsymbol{K}_{fyy}\ {}^3\boldsymbol{K}_{fxx}\ {}^3\boldsymbol{K}_{fyy}\right]^T.$$

Also, x_i and y_i denote the elements of the position vectors directing from the ith finger contact position to

the task position, and they are given to be all positive. ${}^i\boldsymbol{K}_{fxx}$ and ${}^i\boldsymbol{K}_{fyy}$ represent the x- and y-directional stiffness elements in the fingertip space of the ith finger, respectively.

Note that the elements of the second row of the mapping matrix $[\boldsymbol{B}_f^o]$ in (3) are calculated as zero. This is because we excluded the coupling terms ${}^i\boldsymbol{K}_{fxy}(i = 1, 2, 3)$ in the fingertip space for independent compliance control. Thus, we have zero $\boldsymbol{K}_{oxy}$, which, in fact, is a linear combination of ${}^i\boldsymbol{K}_{fxy}(i = 1, 2, 3)$.

Thus, the resultant stiffness matrix in the operational space can be specified as follows:

$$\begin{bmatrix} \boldsymbol{K}_{oxx} & \boldsymbol{K}_{oxy} & \boldsymbol{K}_{ox\phi} \\ \boldsymbol{K}_{oyx} & \boldsymbol{K}_{oyy} & \boldsymbol{K}_{oy\phi} \\ \boldsymbol{K}_{o\phi x} & \boldsymbol{K}_{o\phi y} & \boldsymbol{K}_{o\phi\phi} \end{bmatrix} = \begin{bmatrix} S & 0 & 0, \pm\psi_1 \\ 0 & L & 0, \pm\psi_2 \\ 0, \pm\psi_1 & 0, \pm\psi_2 & S \end{bmatrix}, \tag{4}$$

where ψ_1 and ψ_2 are all positive parameters. And S and L mean that small and large value of stiffness, respectively. The diagonal elements can be determined by considering the task characteristics for each direction[11]-[13]. ψ_1 and ψ_2 can be arbitrarily determined and also those parameters can be suitably adjusted by considering additional control performance(e.g. the jamming effect of assembly tasks).

Next, consider the compliance center lying in the point $\boldsymbol{O}_0$ of Figure 1. In this case, the signs of y_1 and y_2 in the third row of $[\boldsymbol{B}_f^o]$ are changed by moving the compliance center from $\boldsymbol{O}_1$ to $\boldsymbol{O}_0$. Thus, the stiffness matrix in the operational space can be specified as follows[15]:

$$\begin{bmatrix} \boldsymbol{K}_{oxx} & \boldsymbol{K}_{oxy} & \boldsymbol{K}_{ox\phi} \\ \boldsymbol{K}_{oyx} & \boldsymbol{K}_{oyy} & \boldsymbol{K}_{oy\phi} \\ \boldsymbol{K}_{o\phi x} & \boldsymbol{K}_{o\phi y} & \boldsymbol{K}_{o\phi\phi} \end{bmatrix} = \begin{bmatrix} S & 0 & +\psi_1 \\ 0 & L & 0, \pm\psi_2 \\ +\psi_1 & 0, \pm\psi_2 & S \end{bmatrix}, \tag{5}$$

2.2 *Left-angled and Right-angled Pegs*

In this section, we first consider that a multi-fingered hand inserts a left-angled peg into a hole as shown in Figure 2. The stiffness mapping matrix $[\boldsymbol{B}_f^o]$ between the operational space and the fingertip space is given by

$$[\boldsymbol{B}_f^o] = \begin{bmatrix} 0 & 1 & 0 & 1 & 0 & 1 \\ 0 & 0 & 0 & 0 & 0 & 0 \\ 0 & -x_1 & 0 & -x_2 & 0 & -x_3 \\ 1 & 0 & 1 & 0 & 1 & 0 \\ -y_1 & 0 & -y_2 & 0 & -y_3 & 0 \\ y_1^2 & x_1^2 & y_2^2 & x_2^2 & y_3^2 & x_3^2 \end{bmatrix}. \tag{6}$$

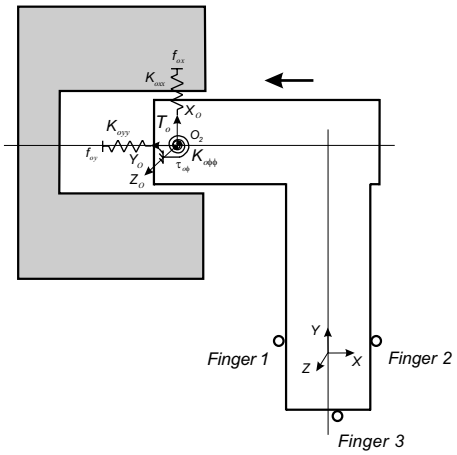

Figure 2: Peg-in-hole task using multi-fingered hands (left-angled peg)

Note that the third and fifth rows of $[\boldsymbol{B}_f^o]$ have zero or minus signs. Also, since the three influence coefficients (i.e., x_i, y_i, $(i = 1, 2, 3)$) are always positive, we can easily notice that $\boldsymbol{K}_{ox\phi}$ and $\boldsymbol{K}_{oy\phi}$ corresponding to the third and fifth rows of $[\boldsymbol{B}_f^o]$ are always calculated as negative values.

Consequently, the stiffness matrix in the operational space can be specified as follows:

$$\begin{bmatrix} \boldsymbol{K}_{oxx} & \boldsymbol{K}_{oxy} & \boldsymbol{K}_{ox\phi} \\ \boldsymbol{K}_{oyx} & \boldsymbol{K}_{oyy} & \boldsymbol{K}_{oy\phi} \\ \boldsymbol{K}_{o\phi x} & \boldsymbol{K}_{o\phi y} & \boldsymbol{K}_{o\phi\phi} \end{bmatrix} = \begin{bmatrix} S & 0 & -\psi_1 \\ 0 & L & -\psi_2 \\ -\psi_1 & -\psi_2 & S \end{bmatrix}. \tag{7}$$

For independent task-space control, it is desirable to have a diagonal operational stiffness matrix. However, the grasping geometry does not allow this objective since $\boldsymbol{K}_{ox\phi}$ and $\boldsymbol{K}_{oy\phi}$ are given negative values. That is, $\boldsymbol{K}_{ox\phi}$ and $\boldsymbol{K}_{oy\phi}$ are not controllable parameters in this grasp configuration. On the other hand, it has been reported that these coupling stiffness elements are very useful to prevent jamming and contact induced vibrations of contact tasks[14], and also useful for effective assembly tasks[16]. They are determined by the following procedures. By rearranging (6), we have the following linear matrix equation:

$$K_{oo}^* = [\boldsymbol{D}_f^o] K_{ff}. \tag{8}$$

where

$$[\boldsymbol{D}_f^o] = \begin{bmatrix} 0 & 1 & 0 & 1 & 0 & 1 \\ 1 & 0 & 1 & 0 & 1 & 0 \\ y_1^2 & x_1^2 & y_2^2 & x_2^2 & y_3^2 & x_3^2 \end{bmatrix},$$

$$[K_{oo}^*] = \begin{bmatrix} \boldsymbol{K}_{oxx} & \boldsymbol{K}_{oyy} & \boldsymbol{K}_{o\phi\phi} \end{bmatrix}.$$

Then, K_{ff} can be obtained by solving (8) and also, the coupling stiffness element ψ_1 and ψ_2 can be determined by

$$\psi_1 = -[\boldsymbol{B}_f^o]_3 \; K_{ff}, \tag{9}$$

$$\psi_2 = -[\boldsymbol{B}_f^o]_5 \; K_{ff}, \tag{10}$$

where $[\boldsymbol{B}_f^o]_i$ denotes the ith row of $[\boldsymbol{B}_f^o]$.

Next, consider that a multi-fingered hand inserts a right-angled peg into a hole as shown in Figure 3.

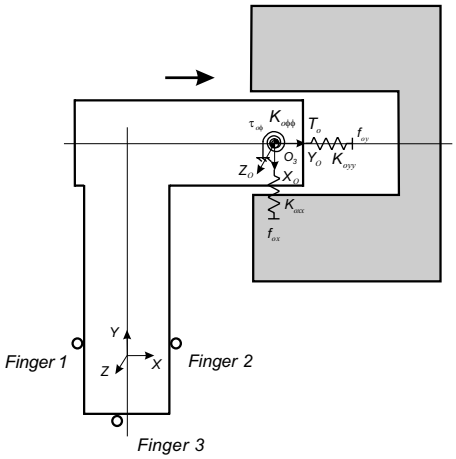

Figure 3: Peg-in-hole task using multi-fingered hands (right-angled peg)

In Figure 3, the stiffness mapping matrix $[\boldsymbol{B}_f^o]$ between the operational space and the fingertip space is given by

$$[\boldsymbol{B}_f^o] = \begin{bmatrix} 0 & 1 & 0 & 1 & 0 & 1 \\ 0 & 0 & 0 & 0 & 0 & 0 \\ 0 & -x_1 & 0 & -x_2 & 0 & -x_3 \\ 1 & 0 & 1 & 0 & 1 & 0 \\ y_1 & 0 & y_2 & 0 & y_3 & 0 \\ y_1^2 & x_1^2 & y_2^2 & x_2^2 & y_3^2 & x_3^2 \end{bmatrix}. \tag{11}$$

Note that the 5th rows of $[\boldsymbol{B}_f^o]$ have all positive signs opposite to the case of a left-angled peg into a hole task. Thus, $\boldsymbol{K}_{oy\phi}$ corresponding to the 5th row of $[\boldsymbol{B}_f^o]$ is always a positive value and the stiffness matrix in the operational space can be specified as follows:

$$\begin{bmatrix} \boldsymbol{K}_{oxx} & \boldsymbol{K}_{oxy} & \boldsymbol{K}_{ox\phi} \\ \boldsymbol{K}_{oyx} & \boldsymbol{K}_{oyy} & \boldsymbol{K}_{oy\phi} \\ \boldsymbol{K}_{o\phi x} & \boldsymbol{K}_{o\phi y} & \boldsymbol{K}_{o\phi\phi} \end{bmatrix} = \begin{bmatrix} S & 0 & -\psi_1 \\ 0 & L & +\psi_2 \\ -\psi_1 & +\psi_2 & S \end{bmatrix}. \tag{12}$$

2.3 *Perpendicular Peg*

This section considers that a perpendicular peg is inserted into a hole by using two hands like human as shown in Figure 4.

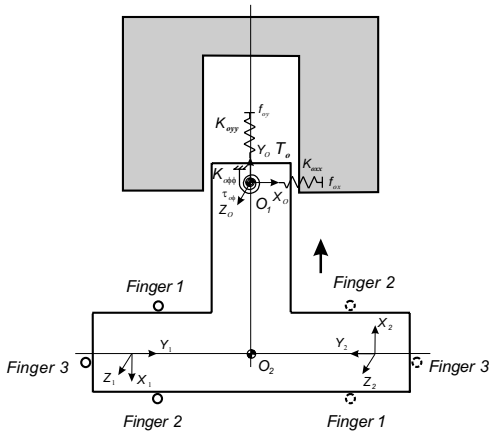

Figure 4: Peg-in-hole task using a two hands (perpendicular peg)

In this case, the stiffness matrix in the operational space can be expressed as

$$[\boldsymbol{K}_o] = \sum_{i=1}^{2} {}^i[\boldsymbol{G}_o^f]^T \; {}^i[\boldsymbol{K}_f] \; {}^i[\boldsymbol{G}_o^f], \tag{13}$$

where ${}^i[\boldsymbol{K}_f]$ and ${}^i[\boldsymbol{G}_o^f]$ denote the stiffness matrix in the fingertip space of the ith hand and the Jacobian matrix relating the fingertip space of the ith hand to the operational space, respectively.

Also, the stiffness mapping matrix $[\boldsymbol{B}_f^o]$ between the operational space and the fingertip space of each hand can be represented by

$$[\boldsymbol{B}_f^o] = \left[{}^1[\boldsymbol{B}_f^o] \;\; {}^2[\boldsymbol{B}_f^o] \right], \tag{14}$$

where ${}^i[\boldsymbol{B}_f^o]$ denotes the stiffness mapping matrix between the operational space and the fingertip space of the ith hand.

When the hand system grasps the peg for the compliance center $\boldsymbol{O}_1$ of Figure 4, this is identical to combine the two cases of Figures 2 and 3. As a result, the coupling stiffness element $\boldsymbol{K}_{oy\phi}$ can be arbitrarily specified, but $\boldsymbol{K}_{ox\phi}$ cannot be arbitrarily planned. If the compliance center is moved to the point $\boldsymbol{O}_2$, the sign of the kinematic influence coefficient y_1 in (6) changes into negative, and the sign of the kinematic influence coefficient y_2 in (11) changes into negative. Also, we can notice that the coupling stiffness element $\boldsymbol{K}_{oy\phi}$ is arbitrarily specified, but $\boldsymbol{K}_{ox\phi}$ still cannot be arbitrarily planned and specifically, $\boldsymbol{K}_{ox\phi}$ is always negative. Consequently, we can note that the x-directional position accuracy is very important for stable assembly tasks.

2.4 *Polishing Task by Belt Sander*

Now, consider a polishing task by belt sander as shown in Figure 5. When an object grasped by multi-

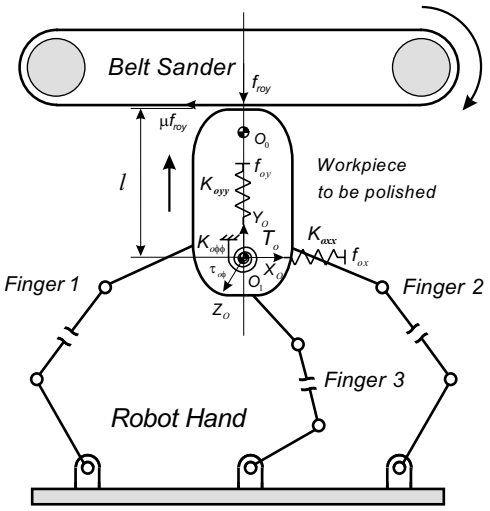

Figure 5: Polishing task of an object by using belt sander

fingered hand is being polished by belt sander, the stiffness matrix in the operational space for the compliance center $\boldsymbol{O}_1$ can be specified by (4). In Figure 5, the forces exerted on the virtual springs attached to the compliance center $\boldsymbol{O}_1$ can be expressed as

$$\begin{bmatrix} f_{ox} \\ f_{oy} \\ \tau_{o\phi} \end{bmatrix} = \begin{bmatrix} \boldsymbol{K}_{oxx} & 0 & \boldsymbol{K}_{ox\phi} \\ 0 & \boldsymbol{K}_{oyy} & \boldsymbol{K}_{oy\phi} \\ \boldsymbol{K}_{o\phi x} & \boldsymbol{K}_{o\phi y} & \boldsymbol{K}_{o\phi\phi} \end{bmatrix} \begin{bmatrix} \delta u_{ox} \\ \delta u_{oy} \\ \delta u_{o\phi} \end{bmatrix}, \quad (15)$$

where the small deflections of the virtual springs in the x-, y-, and ϕ(rotation)-directions, respectively, are given by

$$\begin{aligned} \delta u_{ox} &= u^d_{ox} - u^a_{ox}, \\ \delta u_{oy} &= u^d_{oy} - u^a_{oy}, \\ \delta u_{o\phi} &= u^d_{o\phi} - u^a_{o\phi}, \end{aligned}$$

and here u^d_{oj} and u^a_{oj} denote the desired and actual positions in the j-direction, respectively.

The x-directional force f_{ox}, y-directional force f_{oy}, and torque $\tau_{o\phi}$, which are induced by the y-directional reaction force($f_{roy} > 0$), are given by

$$f_{ox} = -\mu f_{roy}, \quad (16)$$
$$f_{oy} = -f_{roy}, \quad (17)$$
$$\tau_{o\phi} = \mu f_{roy} l, \quad (18)$$

where μ and l denote the friction coefficient at the contacting surface and the length between the compliance center and the polishing point, respectively.

From (15) to (18), the force and torque relations at the compliance center $\boldsymbol{O}_1$ can be obtained as

$$-\mu f_{roy} = \boldsymbol{K}_{oxx}\delta u_{ox} + \boldsymbol{K}_{ox\phi}\delta u_{o\phi}, \quad (19)$$
$$-f_{roy} = \boldsymbol{K}_{oyy}\delta u_{oy} + \boldsymbol{K}_{oy\phi}\delta u_{o\phi}, \quad (20)$$
$$\mu f_{roy} l = \boldsymbol{K}_{o\phi x}\delta u_{ox} + \boldsymbol{K}_{o\phi y}\delta u_{oy} + \boldsymbol{K}_{o\phi\phi}\delta u_{o\phi}. \quad (21)$$

By rearranging (19) and (20), we have

$$\delta u_{ox} = -\frac{\mu f_{roy}}{\boldsymbol{K}_{oxx}} - \frac{\delta u_{o\phi}}{\boldsymbol{K}_{oxx}}\boldsymbol{K}_{ox\phi}, \quad (22)$$
$$\delta u_{oy} = -\frac{f_{roy}}{\boldsymbol{K}_{oyy}} - \frac{\delta u_{o\phi}}{\boldsymbol{K}_{oyy}}\boldsymbol{K}_{oy\phi}. \quad (23)$$

When an object grasped by a multi-fingered hand is polished by pushing the object toward the rotating belt sander, if a virtual desired path to be followed is intentionally given to be inside the surface of the belt sander, the small deflection δu_{ox} of the virtual spring in the x-direction becomes negative by friction force. Thus, the positive orientational change of the grasped object is occurred by the torque caused by the friction force. If the reaction force is excessively increased by unreasonable pushing force, it is desired that the effect by the reaction force is decreased by large negative deflection to the y-direction, and also the x-directional deflection is decreased for stable polishing task. In this sense, the coupling stiffness elements, $\boldsymbol{K}_{ox\phi}$ and $\boldsymbol{K}_{oy\phi}$, should be chosen as negative and positive values for compliant polishing task. On the other hand, when the compliance center is lying in the point $\boldsymbol{O}_0$ in Figure 5, the coupling stiffness element $\boldsymbol{K}_{ox\phi}$ always should be positive. In this case, since the x-directional deflection is increased by the excessive y-directional reaction force, the resultant orientation of the object may be unstable.

Consequently, the following stiffness matrix in the operational space may be a good choice for effective polishing tasks.

$$\begin{bmatrix} \boldsymbol{K}_{oxx} & \boldsymbol{K}_{oxy} & \boldsymbol{K}_{ox\phi} \\ \boldsymbol{K}_{oyx} & \boldsymbol{K}_{oyy} & \boldsymbol{K}_{oy\phi} \\ \boldsymbol{K}_{o\phi x} & \boldsymbol{K}_{o\phi y} & \boldsymbol{K}_{o\phi\phi} \end{bmatrix} = \begin{bmatrix} L & 0 & -\psi_1 \\ 0 & S & +\psi_2 \\ -\psi_1 & +\psi_2 & S \end{bmatrix}. \quad (24)$$

3 Specifying Compliance Characteristics: Three-dimension

3.1 *Left-angled and Right-angled Pegs*

When a multi-fingered hand assembles a straight peg into a hole in three-dimensional space, the stiffness

matrix to be specified in the operational space have to be analyzed[15].

In this section, we first consider that a multi-fingered hand inserts a left-angled peg into a hole as shown in Figure 6. The stiffness relation between the operational space and the fingertip space is given by

$$K_{oo} = [\boldsymbol{B}_f^o]\, K_{ff}$$

$$\begin{bmatrix} \boldsymbol{K}_{oxx} \\ \boldsymbol{K}_{oxy} \\ \boldsymbol{K}_{oxz} \\ \boldsymbol{K}_{ox\gamma} \\ \boldsymbol{K}_{ox\beta} \\ \boldsymbol{K}_{ox\alpha} \\ \boldsymbol{K}_{oyy} \\ \boldsymbol{K}_{oyz} \\ \boldsymbol{K}_{oy\gamma} \\ \boldsymbol{K}_{oy\beta} \\ \boldsymbol{K}_{oy\alpha} \\ \boldsymbol{K}_{ozz} \\ \boldsymbol{K}_{oz\gamma} \\ \boldsymbol{K}_{oz\beta} \\ \boldsymbol{K}_{oz\alpha} \\ \boldsymbol{K}_{o\gamma\gamma} \\ \boldsymbol{K}_{o\gamma\beta} \\ \boldsymbol{K}_{o\gamma\alpha} \\ \boldsymbol{K}_{o\beta\beta} \\ \boldsymbol{K}_{o\beta\alpha} \\ \boldsymbol{K}_{o\alpha\alpha} \end{bmatrix} = \begin{bmatrix} 0 & 0 & 1 & 0 & 0 & 1 & 0 & 0 & 1 & 0 & 0 & 1 \\ 0 & 0 & 0 & 0 & 0 & 0 & 0 & 0 & 0 & 0 & 0 & 0 \\ 0 & 0 & 0 & 0 & 0 & 0 & 0 & 0 & 0 & 0 & 0 & 0 \\ 0 & 0 & 0 & 0 & 0 & 0 & 0 & 0 & 0 & 0 & 0 & 0 \\ 0 & 0 & x_1 & 0 & 0 & x_2 & 0 & 0 & x_3 & 0 & 0 & x_4 \\ \hline 0 & 0 & -y_1 & 0 & 0 & y_2 & 0 & 0 & -y_3 & 0 & 0 & y_4 \\ 0 & 1 & 0 & 0 & 1 & 0 & 0 & 1 & 0 & 0 & 1 & 0 \\ 0 & 0 & 0 & 0 & 0 & 0 & 0 & 0 & 0 & 0 & 0 & 0 \\ 0 & -x_1 & 0 & 0 & -x_2 & 0 & 0 & -x_3 & 0 & 0 & -x_4 & 0 \\ \hline 0 & 0 & 0 & 0 & 0 & 0 & 0 & 0 & 0 & 0 & 0 & 0 \\ 0 & -z_1 & 0 & 0 & -z_2 & 0 & 0 & -z_3 & 0 & 0 & -z_4 & 0 \\ \hline 1 & 0 & 0 & 1 & 0 & 0 & 1 & 0 & 0 & 1 & 0 & 0 \\ y_1 & 0 & 0 & -y_2 & 0 & 0 & y_3 & 0 & 0 & -y_4 & 0 & 0 \\ z_1 & 0 & 0 & z_2 & 0 & 0 & z_3 & 0 & 0 & z_4 & 0 & 0 \\ \hline 0 & 0 & 0 & 0 & 0 & 0 & 0 & 0 & 0 & 0 & 0 & 0 \\ y_1^2 & x_1^2 & 0 & y_2^2 & x_2^2 & 0 & y_3^2 & x_3^2 & 0 & y_4^2 & x_4^2 & 0 \\ y_1 z_1 & 0 & 0 & -y_2 z_2 & 0 & 0 & y_3 z_3 & 0 & 0 & -y_4 z_4 & 0 & 0 \\ 0 & x_1 z_1 & 0 & 0 & x_2 z_2 & 0 & 0 & x_3 z_3 & 0 & 0 & x_4 z_4 & 0 \\ \hline z_1^2 & 0 & x_1^2 & z_2^2 & 0 & x_2^2 & z_3^2 & 0 & x_3^2 & z_4^2 & 0 & x_4^2 \\ 0 & 0 & -x_1 y_1 & 0 & 0 & x_2 y_2 & 0 & 0 & -x_3 y_3 & 0 & 0 & x_4 y_4 \\ 0 & z_1^2 & y_1^2 & 0 & z_2^2 & y_2^2 & 0 & z_3^2 & y_3^2 & 0 & z_4^2 & y_4^2 \end{bmatrix}$$

$$\begin{bmatrix} 0 & 0 & 1 \\ 0 & 0 & 0 \\ 0 & 0 & 0 \\ 0 & 0 & 0 \\ 0 & 0 & x_5 \\ \hline 0 & 0 & -y_5 \\ 0 & 1 & 0 \\ 0 & 0 & 0 \\ 0 & -x_5 & 0 \\ \hline 0 & 0 & 0 \\ 0 & -z_5 & 0 \\ \hline 1 & 0 & 0 \\ y_5 & 0 & 0 \\ z_5 & 0 & 0 \\ \hline 0 & 0 & 0 \\ y_5^2 & 0 & x_5^2 \\ y_5 z_5 & 0 & 0 \\ 0 & x_5 z_5 & 0 \\ \hline z_5^2 & 0 & x_5^2 \\ 0 & 0 & -x_5 y_5 \\ 0 & z_5^2 & y_5^2 \end{bmatrix} \begin{bmatrix} {}^1\boldsymbol{K}_{fxx} \\ {}^1\boldsymbol{K}_{fyy} \\ {}^1\boldsymbol{K}_{fzz} \\ {}^2\boldsymbol{K}_{fxx} \\ {}^2\boldsymbol{K}_{fyy} \\ {}^2\boldsymbol{K}_{fzz} \\ {}^3\boldsymbol{K}_{fxx} \\ {}^3\boldsymbol{K}_{fyy} \\ {}^3\boldsymbol{K}_{fzz} \\ {}^4\boldsymbol{K}_{fxx} \\ {}^4\boldsymbol{K}_{fyy} \\ {}^4\boldsymbol{K}_{fzz} \\ {}^5\boldsymbol{K}_{fxx} \\ {}^5\boldsymbol{K}_{fyy} \\ {}^5\boldsymbol{K}_{fzz} \end{bmatrix}, \quad (25)$$

where x_i, y_i, and z_i denote the elements of position vectors directing from the ith finger contact position to the task position, and they are given to be all positive. ${}^i\boldsymbol{K}_{fxx}$, ${}^i\boldsymbol{K}_{fyy}$, and ${}^i\boldsymbol{K}_{fzz}$ represent the x-, y-, and z-directional stiffness elements in the fingertip space of the ith finger, respectively.

In (25), all elements of $[\boldsymbol{B}_f^o]_5$, $[\boldsymbol{B}_f^o]_9$, $[\boldsymbol{B}_f^o]_{11}$, $[\boldsymbol{B}_f^o]_{14}$, and $[\boldsymbol{B}_f^o]_{18}$ have the same signs, respectively, where $[\boldsymbol{B}_f^o]_i$ denotes the ith row of $[\boldsymbol{B}_f^o]$. Therefore, the stiffness elements $\boldsymbol{K}_{ox\beta}$, $\boldsymbol{K}_{oy\gamma}$, $\boldsymbol{K}_{oy\alpha}$, $\boldsymbol{K}_{z\beta}$, and $\boldsymbol{K}_{o\gamma\alpha}$ cannot be arbitrarily planned.

Consequently, the stiffness matrix in the operational space can be specified as follows:

$$\begin{bmatrix} \boldsymbol{K}_{oxx} & \boldsymbol{K}_{oxy} & \boldsymbol{K}_{oxz} & \boldsymbol{K}_{ox\gamma} & \boldsymbol{K}_{ox\beta} & \boldsymbol{K}_{ox\alpha} \\ \boldsymbol{K}_{oyx} & \boldsymbol{K}_{oyy} & \boldsymbol{K}_{oyz} & \boldsymbol{K}_{oy\gamma} & \boldsymbol{K}_{oy\beta} & \boldsymbol{K}_{oy\alpha} \\ \boldsymbol{K}_{ozx} & \boldsymbol{K}_{ozy} & \boldsymbol{K}_{ozz} & \boldsymbol{K}_{oz\gamma} & \boldsymbol{K}_{oz\beta} & \boldsymbol{K}_{oz\alpha} \\ \boldsymbol{K}_{o\gamma x} & \boldsymbol{K}_{o\gamma y} & \boldsymbol{K}_{o\gamma z} & \boldsymbol{K}_{o\gamma\gamma} & \boldsymbol{K}_{o\gamma\beta} & \boldsymbol{K}_{o\gamma\alpha} \\ \boldsymbol{K}_{o\beta x} & \boldsymbol{K}_{o\beta y} & \boldsymbol{K}_{o\beta z} & \boldsymbol{K}_{o\beta\gamma} & \boldsymbol{K}_{o\beta\beta} & \boldsymbol{K}_{o\beta\alpha} \\ \boldsymbol{K}_{o\alpha x} & \boldsymbol{K}_{o\alpha y} & \boldsymbol{K}_{o\alpha z} & \boldsymbol{K}_{o\alpha\gamma} & \boldsymbol{K}_{o\alpha\beta} & \boldsymbol{K}_{o\alpha\alpha} \end{bmatrix} =$$

$$\begin{bmatrix} S & 0 & 0 & 0 & +\psi_1 & 0, \pm\psi_2 \\ 0 & S & 0 & -\psi_3 & 0 & -\psi_4 \\ 0 & 0 & L & 0, \pm\psi_5 & +\psi_6 & 0 \\ 0 & -\psi_3 & 0, \pm\psi_5 & S & 0, \pm\psi_7 & +\psi_8 \\ +\psi_1 & 0 & +\psi_6 & 0, \pm\psi_7 & S & 0, \pm\psi_9 \\ 0, \pm\psi_2 & -\psi_4 & 0 & +\psi_8 & 0, \pm\psi_9 & L \end{bmatrix} \quad (26)$$

where $\psi_i (i = 1, 2, \cdots, 9)$ are all positive parameters. And S and L mean that small and large value of stiffness, respectively. The diagonal elements can be determined by considering the control characteristics for each direction[11]-[13].

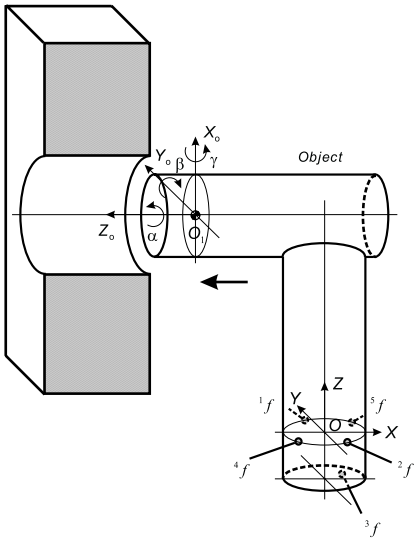

Figure 6: Peg-in-hole task using multi-fingered hands in three-dimensional space(left-angled peg)

In (26), $\psi_i (i = 2, 5, 7, 9)$ can be arbitrarily determined and also those parameters can be suitably adjusted by considering additional control performance(e.g. the jamming effect of assembly tasks). On the other hand, $\psi_j (j = 1, 3, 4, 6, 8)$ can be determined by the following procedures. Let $[\boldsymbol{D}_f^o](10 \times 21)$ be the matrix excluding the rows of $[\boldsymbol{B}_f^o]_i (i = 2, 3, 4, 5, 8, 9, 10, 11, 14, 15, 18)$, and K_{oo}^* in (25), and $K_{oo}^* (10 \times 1)$ be the vector excluding $\boldsymbol{K}_{oxy}$, $\boldsymbol{K}_{oxz}$, $\boldsymbol{K}_{ox\gamma}$, $\boldsymbol{K}_{ox\beta}$, $\boldsymbol{K}_{oyz}$, $\boldsymbol{K}_{oy\gamma}$, $\boldsymbol{K}_{oy\beta}$, and $\boldsymbol{K}_{oz\alpha}$ of K_{oo}. Then, K_{ff} can be obtained by solving the following linear matrix equation:

$$K_{oo}^* = [\boldsymbol{D}_f^o] K_{ff}. \tag{27}$$

Then, the coupling stiffness elements $\psi_j (j = 1, 3, 4, 6, 8)$ can be determined by

$$\psi_1 = [\boldsymbol{B}_f^o]_5 \; K_{ff}, \tag{28}$$

$$\psi_3 = -[\boldsymbol{B}_f^o]_9 \; K_{ff}, \tag{29}$$

$$\psi_4 = -[\boldsymbol{B}_f^o]_{11} \; K_{ff}, \tag{30}$$

$$\psi_6 = [\boldsymbol{B}_f^o]_{14} \; K_{ff}, \tag{31}$$

and

$$\psi_8 = [\boldsymbol{B}_f^o]_{18} \; K_{ff}. \tag{32}$$

Now, consider that a multi-fingered hand inserts a right-angled peg into a hole as shown in Figure 7. In this case, the signs of all $z_i (i = 1, \cdots, 5)$ in (25) are changed into negative. Thus, we can notice that the coupling stiffness elements $\boldsymbol{K}_{oy\alpha}$, $\boldsymbol{K}_{oz\beta}$ and $\boldsymbol{K}_{o\gamma\alpha}$ cannot be arbitrarily planned and also their signs changes from positive to negative or vice versa in comparison to the previous case.

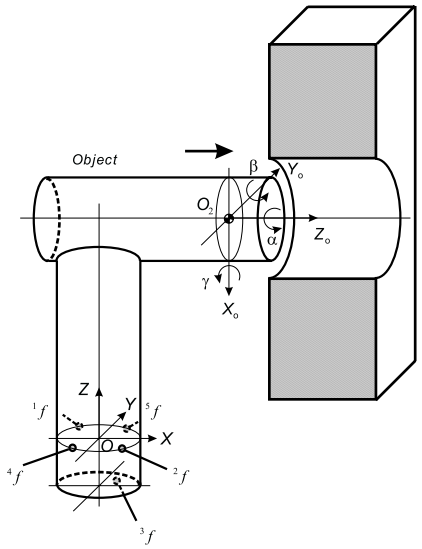

Figure 7: Peg-in-hole task using multi-fingered hands in three-dimensional space(right-angled peg)

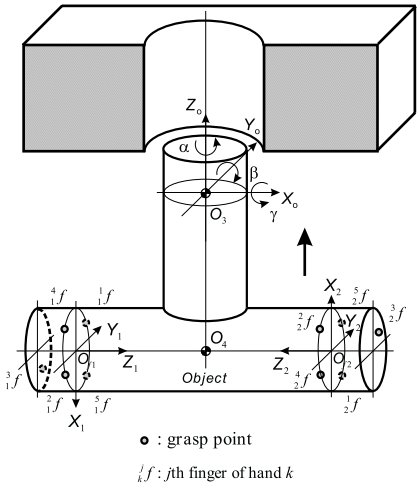

Figure 8: Peg-in-hole task using multi-fingered hands in three-dimensional space(perpendicular peg)

3.2 *Perpendicular Peg*

When the hand grasps the left-side of the peg and the compliance center lies in the point $\boldsymbol{O}_3$ of Figure 8, we can identically analyze the stiffness relation between the operational space and the fingertip space

similar to the case of Figure 6. Also, if the hand grasps the right-side of the peg for the same compliance center $\boldsymbol{O}_3$, we can identically analyze the stiffness relation between the operational space and the fingertip space as the case of Figure 7.

On the other hand, when the hand grasps the left-side of the peg and the compliance center is moved to the point $\boldsymbol{O}_4$, the sign of the kinematic influence coefficients z_1 and z_4 in (25) changes from positive to negative or vice versa. Also, if the hand grasps the right-side of the peg for the same compliance center $\boldsymbol{O}_4$, the sign of the kinematic influence coefficients z_1, z_3, and z_4 in (25) changes from positive to negative or vice versa. Thus, we can notice that the coupling stiffness elements $\boldsymbol{K}_{oy\alpha}$, $\boldsymbol{K}_{oz\beta}$ and $\boldsymbol{K}_{o\gamma\alpha}$ can be arbitrarily specified, but $\boldsymbol{K}_{ox\beta}$ and $\boldsymbol{K}_{oy\gamma}$ still cannot be arbitrarily planned in those cases. Specifically, $\boldsymbol{K}_{ox\beta}$ is always positive, and $\boldsymbol{K}_{oy\gamma}$ is always negative.

As a result, in assembly tasks using multi-fingered hands, we can conclude that the compliance characteristics in the operational space should be differently applied according to the grasp geometry and also, it is closely associated with the compliance center.

4 Concluding Remarks

A guideline of specifying compliance characteristics in the operational space of multi-fingered hands was analyzed in this paper. Through analyzing the stiffness relation between the operational space and the fingertip space of multi-fingered hands, it is shown that some stiffness elements in the operational space are appropriately planned, but some of coupling stiffness elements cannot be planned arbitrarily. As a result, we confirmed that five-fingered hands can modulate the six-degree of freedom operational compliance characteristics by using an independent finger-based compliance control method[15]. Also, we can notice that the operational stiffness matrix should be carefully specified by considering the grasp geometry of multi-fingered hands for successful grasping and manipulation tasks.

References

[1] T. Yoshikawa, and X. -Z. Zheng, "Coordinated dynamic hybrid position/force control for multiple robot manipulators handling one constrained object," *Int. Jour. of Robotics Research*, Vol. 12, No. 3, pp. 219-230, 1993.

[2] H. Maekawa, K. Tanie, and K. Komoria, "Dynamic grasping force control using tactile feedback for grasp of multifingered hand," *Proc. of IEEE Int. Conf. on Robotics and Automation*, pp. 2462-2469, April 1996.

[3] S. L. Jiang, K. K. Choi, and Z. X. Li, "Coordinated motion generation for multifingered manipulation using tactile feedback," *Proc. of IEEE Int. Conf. on Robotics and Automation*, pp. 3032-3037, May 1999.

[4] J. L. Pons, R. Ceres, and F, Pfeiffer, "Multifingered dexterous robotics hand design and control: a review," *Robotica*, Vol. 17, pp. 661-674, 1999.

[5] M. R. Cutkosky, and I. Kao, "Computing and controlling the compliance of a robotic hand," *IEEE Trans. on Robotics and Automation*, Vol. 5, No. 2, pp. 151-165, 1989.

[6] I. Kao, M. R. Cutkosky, and R. S. Johansson, "Robotic stiffness control and calibration as applied to humnan grasping tasks," *IEEE Trans. on Robotics and Automation*, Vol. 13, No. 4, pp. 557-566, 1997.

[7] D. E. Whitney, "Quasi-static assembly of compliantly supported rigid parts," *Jour. of Dynamic systems, Measurement, and control*, Vol. 104, pp. 65-77, March 1982.

[8] H. Asada, Y. Kakumoto, "The dynamic analysis and design of a high-speed insertion hand using the generalized centroid and virtual mass," *Jour. of Dynamic systems, Measurement, and control*, Vol. 112, pp. 646-652, 1990.

[9] T. Matsuoka, T. Hasegawa, T. Kiriki, and K, Honda, "Mechanical assembly based on motion primitives of multi-fingered hand," *Proc. of Advanced Intelligent Mechatronics*, 1997.

[10] B. -H. Kim, B. -J. Yi, I. H. Suh, and S. -R. Oh, "A biomimetic compliance control of robot hand by considering structures of human finger," *Proc. of IEEE Int. Conf. on Robotics and Automation*, pp. 3880-3887, 2000.

[11] J. D. Schutter and H. V. Brussel, "Compliant robot motion I. A formalism for specifying compliant motion tasks," *Int. Jour. of Robotics Research*, vol. 7, no. 4, pp. 3-17, 1988.

[12] J. D. Schutter and H. V. Brussel, "Compliant robot motion II. A control approach based on external control loops," *Int. Jour. of Robotics Research*, vol. 7, no. 4, pp. 18-33, 1988.

[13] K. B. Shimoga and A. A. Goldenberg, "Grasp admittance center: choosing admittance center parameters," *Proc. of American Control Conference*, pp. 2527-2532, 1991.

[14] M. H. Ang, Jr. and G. B. Andeen, "Specifying and achieving passive compliance based on manipulator structure," *IEEE Trans. on Robotics and Automation*, Vol. 11, No. 4, pp. 504-515, 1995.

[15] B. -H. Kim, B. -J. Yi, S. -R. Oh, and I. H. Suh, "Fundamentals and analysis of compliance characteristics for multi-fingered hands," *submitted to the IEEE Int. Conf. on Robotics and Automation*, May 2001.

[16] B. -H. Kim, B. -J. Yi, I. H. Suh, and S. -R. Oh, "Stiffness analysis for effective peg-in/out-hole tasks using multi-fingered robot hands," *to be published in the proc. of IEEE/RSJ Int. Conf. on Intelligent Robots and Systems*, Nov., 2000.